Materials Letters 275 (2020) 128149

Contents lists available at ScienceDirect

Materials Letters

journal homepage: www.elsevier.com/locate/mlblue

Novel low-permittivity microwave dielectric ceramics in garnet-type $Ca_4ZrGe_3O_{12}$

Congxue Su [a,b,*], Laiyuan Ao [c], Yifan Zhai [a], Zhiwei Zhang [a,b], Ying Tang [a,b,*], Junqi Chen [a], Laijun Liu [a], Liang Fang [a,b,c,*]

[a] Guangxi Key Laboratory of Optical and Electronic Materials and Devices, College of Material Science and Engineering, Guilin University of Technology, Guilin 541004, China
[b] Key Laboratory of Nonferrous Materials and New Processing Technology, Ministry of Education, Guilin University of Technology, Guilin 541004, China
[c] College of Materials and Chemical Engineering, Key Laboratory of Inorganic Nonmetallic Crystalline and Energy Conversion Materials, China Three Gorges University, Yichang 443002, China

ARTICLE INFO

Article history:
Received 7 May 2020
Received in revised form 4 June 2020
Accepted 10 June 2020
Available online 13 June 2020

Keywords:
Ceramics
Crystal structure
Dielectrics
Raman
$Ca_4ZrGe_3O_{12}$

ABSTRACT

Novel low-permittivity microwave dielectric ceramics $Ca_4ZrGe_3O_{12}$ with garnet structure were fabricated by a traditional solid-state route. A part of the Ca^{2+} cations are located at the octahedral sites, a quite unusual coordination for this cation in oxygen compounds. The structural characteristics and vibrational modes for the ceramics were studied based on structure refinement and Raman spectra analysis. Owning to the octahedral site is occupied by equivalent Ca^{2+} and Zr^{4+} simultaneously, the deviation between ε_{theo} and ε_r could be related to the rattling effect of smaller Zr^{4+} in the octahedron. Optimum microwave dielectric properties were obtained for $Ca_4ZrGe_3O_{12}$ ceramic sintered at 1340 °C with ε_r = 10.68, $Q \times f$ = 76900 GHz, and τ_f = −41.3 ppm/°C.

1. Introduction

5th generation (5G) mobile communications have been vastly investigated on account of their low time delay, large bandwidths and high-speed data transfer, those desirable characteristics are expected to pave the way for many services such as intelligent transport systems, global positioning systems, and Internet of things [1,2]. In 5G communications, low permittivity (ε_r < 15) and low dielectric loss (high quality factor $Q \times f$) are of great importance for low time delay and large bandwidths. Hence, to meet the emerging requirements, the desire for exploring new microwave dielectric materials with low ε_r and high $Q \times f$ is in the process.

Garnet-type microwave dielectric ceramics with low permittivity have received increasing attentions in the recent decade [3–5]. Garnet structure compounds possess a cubic symmetry of space group $Ia\bar{3}d$ and can be described by the general formula $A_3B_2C_3O_{12}$. Owing to a wide variety of cations in an open framework, different kinds of garnet structure microwave dielectrics including Li-, Ga-, Si-, and V-based materials have been developed [3–6]. Nevertheless, the microwave dielectric properties have been seldom discussed in germanates with garnet structure. Blasse et al. reported the preparation and luminescence of garnet $Ca_4ZrGe_3O_{12}$ in 1995 [7]. The structure refinement of $Ca_4ZrGe_3O_{12}$ was subsequently studied by Zhuravlev et al. [8]. In more recent years, $Ca_4ZrGe_3O_{12}$ compounds were only investigated as potential optically active materials [9]. However, to our knowledge, no research on microwave dielectric properties of $Ca_4ZrGe_3O_{12}$ has been reported. Besides, considering a part of the Ca^{2+} cations are located on the octahedral sites in $Ca_4ZrGe_3O_{12}$, a quite unusual coordination for this cation in oxygen compounds. It's interesting to investigate the microwave dielectric properties of $Ca_4ZrGe_3O_{12}$, and the structural characteristics, Raman vibrational modes for $Ca_4ZrGe_3O_{12}$ ceramics are discussed in this work.

2. Experimental procedures

$Ca_4ZrGe_3O_{12}$ ceramics were synthesized by conventional solid-state ceramic route. Oxide and carbonate powders of $CaCO_3$, ZrO_2, and GeO_2 (99.99%, Aladdin Biological Technology Co. Ltd., Shanghai, China) were weighed stoichiometrically and ball-milled in alcohol for 6 h. The mixture was dried and calcined at 1200 °C for 4 h afterwards. The calcined samples were milled in

* Corresponding authors Guangxi Key Laboratory of Optical and Electronic Materials and Devices, College of Material Science and Engineering, Guilin University of Technology, Guilin 541004, China.
E-mail addresses: alpes1987@163.com (C. Su), tangyinggl001@aliyun.com (Y. Tang), fangliangg1001@aliyun.com (L. Fang).

https://doi.org/10.1016/j.matlet.2020.128149
0167-577X/

alcohol for 8 h. Then the powders were pressed into cylinders under a pressure of 100 MPa with 5 wt% PVA. Finally, these cylinders were sintered at 1280–1360 °C for 6 h in crucibles.

Phase composition of the sintered samples was studied by X-ray diffraction using Panalytical X'pert Pro diffractometer with Cu Kα radiation. Bulk densities of ceramics were measured through Archimedes method. The morphology of sample was analyzed by using Hitachi S4800 scanning electron microscope. The Raman spectra were recorded at room temperature by using a Raman spectrometer (Thermo Fisher Scientific DXR, America) with a 532 nm line in the range of 100–1200 cm^{-1}. The microwave dielectric properties were measured by an Agilent N5230A network analyzer and a Delta 9039 oven. The temperature coefficient of resonant frequency (τ_f) was calculated in the temperature range from 25 °C to 85 °C.

3. Results and discussions

Fig. 1 (a) presents the X-ray diffraction patterns of $Ca_4ZrGe_3O_{12}$ ceramics sintered at various temperatures. All ceramics crystallized into a pure cubic garnet structure without any trace of impurity phases. Rietveld refinement of $Ca_4ZrGe_3O_{12}$ ceramics sintered within the temperature range of 1280–1360 °C from XRD data was carried out by FullProf Suite program. According to Zhuravlev's study [8], the crystal structure of $Ca_3Sn_2SiGa_2O_{12}$ was selected as pristine model in the present work, and the corresponding refinement result is shown in Table 1. The reliable factors confirmed that pure garnet phase with the space group *Ia–3d* was obtained. Fig. 1 (b) shows the Rietveld refinement plots of the 1340 °C-sintered sample. A dense microstructure with clear grain boundaries could be observed for the ceramic sintered at 1340 °C from the inset of Fig. 1 (b). Fig. 1 (c) displays the schematic representation of $Ca_4ZrGe_3O_{12}$. The [GeO_4] tetrahedrons and [$Ca2/ZrO_6$] octahedrons share corners or edges with [$Ca1O_8$] dodecahedrons, forming a three dimensional network. Fig. 1 (d) exhibits the Raman spectra of $Ca_4ZrGe_3O_{12}$ ceramics. As expounded in the previous studies [10,11], the weak peaks at 126 cm^{-1}, 163 cm^{-1} and 258 cm^{-1} could be associated with the translational modes of Ca^{2+} (24c), Ca^{2+}/Zr^{4+} (16a) and Ge(24d)O_4^{4-} sites. The rotational modes of the [GeO_4] tetrahedron are observed at 318 cm^{-1} and the peaks at 440 cm^{-1}, 469 cm^{-1}, 662 cm^{-1} and 684 cm^{-1} are related to the asymmetric Ge-O bending vibrations. The frequencies of 700 ~ 900 cm^{-1} are attributed to the symmetric stretching vibration of the [GeO_4] tetrahedron. The Raman peaks (163, 788 and 816 cm^{-1}) firstly shifted toward low frequency and then shifted toward high frequency with the increasing temperature (details in supplementary information). Besides, the Raman shift of stretching vibration (at 788 cm^{-1}) was closely associated with the variation in the volume of [GeO_4] tetrahedron (details in supplementary information).

Fig. 2 (a) exhibits the relative density of $Ca_4ZrGe_3O_{12}$ ceramics sintered at different temperatures. The relative density firstly increased with the increase of sintering temperature, reaching a maximum value of 98.04% at 1340 °C, and then decreased to 97.03% at 1360 °C. The variation in ε_r was consistent with the density and higher density corresponded to higher ε_r. According to the Bosman and Havinga's correction, $Ca_4ZrGe_3O_{12}$ ceramic sintered at 1340 °C posessed the $\varepsilon_{corrected}$ of 10.99 [12]. The theoretical permittivity ε_{theo} calculated by the Clausius–Mossotti equation and additive rule was 9.19, which was lower than the measured ε_r of 10.68 [13]. The deviation between ε_{theo} and ε_r could be related to the rattling effect of smaller Zr^{4+}, as Shannon pointed out, large dielectric

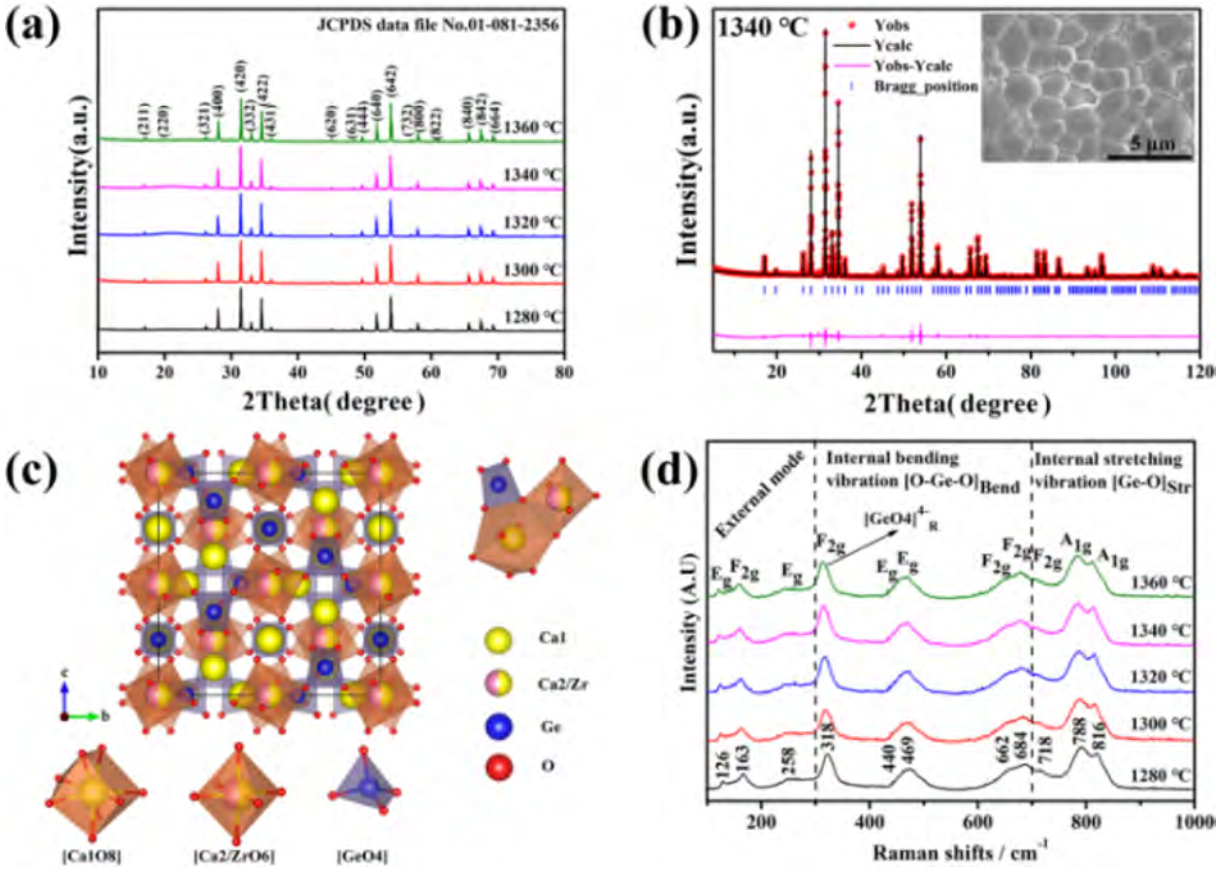

Fig. 1. (a) X-ray diffraction patterns of the $Ca_4ZrGe_3O_{12}$ ceramics; (b) XRD profile of $Ca_4ZrGe_3O_{12}$ ceramic sintered at 1340 °C after fitting, with the SEM image in the inset; (c) crystal structure of $Ca_4ZrGe_3O_{12}$; (d) Raman spectra of $Ca_4ZrGe_3O_{12}$ ceramics.

Table 1
Refinement parameters and reliability of $Ca_4ZrGe_3O_{12}$ ceramics with different sintering temperatures.

T(°C)	Lattice parameters		R_{wp}	R_p	χ^2
	$a = b = c$ (Å)	Cell volume (Å^3)			
1280	12.7102	2053.35	10.9	8.1	3.86
1300	12.7107	2053.58	10.1	7.58	3.18
1320	12.7114	2053.92	9.76	7.56	2.92
1340	12.7134	2054.90	10.5	8.24	2.47
1360	12.7121	2054.26	10.1	7.78	2.48

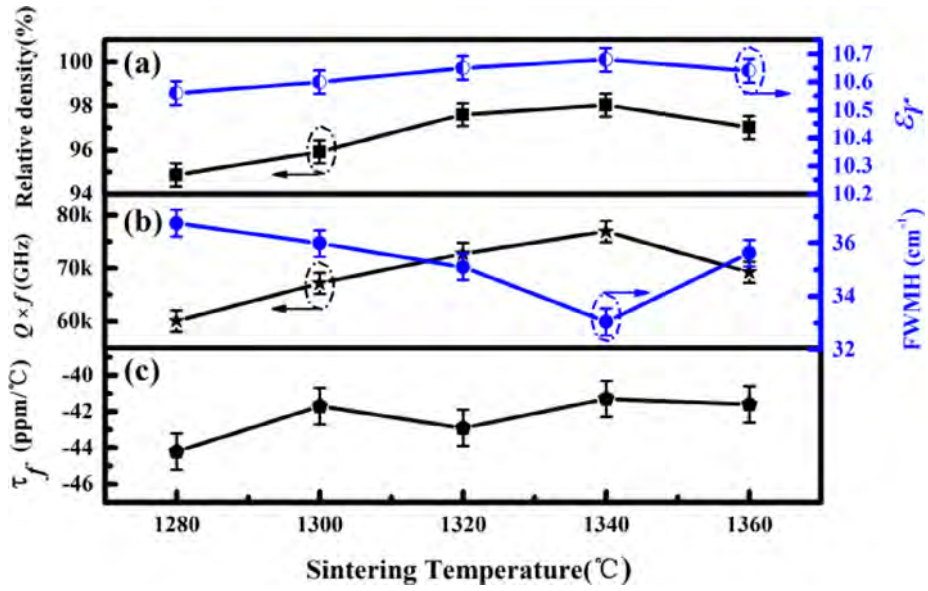

Fig. 2. (a) The relationship between relative density and ε_r of $Ca_4ZrGe_3O_{12}$ ceramics, (b) the relationship between $Q \times f$ and FWHM of A_{1g} mode at 788 cm^{-1}. (c) the τ_f of $Ca_4ZrGe_3O_{12}$ ceramics sintered at different temperatures.

Table 2
Bond valences and bond length of cations in $Ca_4ZrGe_3O_{12}$ ceramic (sintered at 1340 °C for 6 h).

Wyckoff sites	M−O	Number of M−O	Bond length (Å)	Bond valence (Å)
24c	Ca1–O	8	2.5490 and 2.4446	1.93
16a	Ca2–O	6	2.1799	3.3750
16a	Zr–O	6	2.1799	3.1122
24d	Ge–O	4	1.7788	3.6808

deviation (Δ% = 13–34%) can be the presence of rattling cations [13]. Due to the ion radii of Ca^{2+} (1 Å, CN = 6) is much bigger than that of Zr^{4+} (0.72 Å, CN = 6), in order to maintain an undistorted octahedral site in garnet structure, the [ZrO_6] octahedron would change its configuration, resulting in the expansion of volume and the higher polarizability. This conclusion could be verified by calculating the bond valences. The bond length and bond valences of $Ca_4ZrGe_3O_{12}$ ceramic sintered at 1340 °C are listed in Table 2. It is clearly found that the "rattling" Zr^{4+} cations in the octahedrons with smaller bond valence could lead to the large cation polarizabilities.

The relationship between the $Q \times f$ values and the Raman full width at half maximum (FWHM) is illustrated in Fig. 2 (b). Generally, symmetric stretching vibrations in high frequencies (such as A_{1g} peaks at 788 cm^{-1} in this work) often exhibit the strongest intensity in Raman scattering, and the FWHM of these strongest modes are often used to correlate the $Q \times f$ [14,15]. It can be seen that an inverse trend between FWHM of A_{1g} modes (at 788 cm^{-1}) and $Q \times f$ with the increase of sintering temperature. In general, FWMH of A_{1g} mode are the important characterization for the ordering degree in crystal structure, and a narrow FWHM means a high degree of ordering, which is conducive to the higher value of $Q \times f$ [15]. The τ_f values fluctuated around −42 ppm/ °C for ceramics sintered from 1280 °C to 1360 °C, with weak dependence on sintering temperature (Fig. 2 (c)).

4. Conclusions

Novel microwave dielectric ceramics $Ca_4ZrGe_3O_{12}$ with garnet structure were fabricated by solid-state reaction process. Raman spectra of $Ca_4ZrGe_3O_{12}$ ceramics were assigned in terms of external and internal modes. Owning to the octahedral sites are occupied by Ca^{2+} and Zr^{4+} simultaneously, the deviation between ε_{theo} and ε_r might be related to the rattling effect of smaller Zr^{4+} in the octahedral sites. $Ca_4ZrGe_3O_{12}$ ceramic showed optimal dielectric performances with ε_r = 10.68, $Q \times f$ = 76900 GHz, τ_f = − 41.3 ppm/°C when sintered at 1340 °C for 6 h.

CRediT authorship contribution statement

Congxue Su: Conceptualization, Data curation, Formal analysis, Funding acquisition, Investigation, Methodology, Project

administration, Software, Supervision, Validation, Visualization, Writing - original draft, Writing - review & editing. **Laiyuan Ao:** Data curation, Formal analysis, Software, Supervision, Visualization. **Yifan Zhai:** Software, Visualization, Investigation. **Zhiwei Zhang:** Data curation, Formal analysis, Investigation. **Ying Tang:** Funding acquisition, Resources. **Junqi Chen:** Investigation, Writing – review. **Laijun Liu:** Funding acquisition. **Liang Fang:** Conceptualization, Methodology, Project administration, Resources, Writing – review.

Declaration of Competing Interest

The authors declare that they have no known competing financial interests or personal relationships that could have appeared to influence the work reported in this paper.

Acknowledgments

This work was supported by Natural Science Foundation of China (Nos. 21965009 and 21761008), the Natural Science Foundation of Guangxi Zhuang Autonomous Region (Nos. 2018GXNSFBA281093 and 2018GXNSFAA138175), and Projects of Department of Science and Technology of Guangxi (Nos. AA18118008, AA18118034 and AA18118023), and High level innovation team and outstanding scholar program of Guangxi institutes and Innovation Project of Guangxi Graduate Education YCBZ2020066.

Appendix A. Supplementary data

Supplementary data to this article can be found online at https://doi.org/10.1016/j.matlet.2020.128149.

References

[1] Z.Y. Tan, K.X. Song, H.B. Bafrooei, B. Liu, J. Wu, J.M. Xu, H.X. Lin, D.W. Wang, Ceram. Int. 46 (2020) 15665–15669.
[2] Q.B. Lin, K.X. Song, B. Liu, H.B. Bafrooei, D. Zhou, W.T. Su, F. Shi, D.W. Wang, H. X. Lin, I.M. Reaney, Ceram. Int. 46 (2020) 1171–1177.
[3] L. Fang, C.X. Su, H.F. Zhou, Z.H. Wei, H. Zhang, J. Am. Ceram. Soc. 96 (2013) 688–690.
[4] G.G. Yao, C.J. Pei, P. Liu, J.P. Zhou, H.W. Zhang, J. Eur. Ceram. Soc. 34 (2014) 2983–2987.
[5] J.C. Kin, M.H. Kim, S.H. Nahm, J.H. Paik, J.H. Kim, H.J. Lee, J. Eur. Ceram. Soc. 27 (2007) 2865–2870.
[6] J.B. Song, K.X. Song, J.S. Wei, H.X. Lin, J. Wu, J.M. Xu, W.T. Su, Z.Q. Cheng, J. Am. Ceram. Soc. 101 (2018) 244–251.
[7] G. Blasse, J.D. Blank, Mater. Res. Bull. 30 (1995) 845–850.
[8] V.D. Zhuravlev, A.P. Tyutyunnik, N.I. Lobachevskaya, Powder. Diffr. 31 (2016) 292–294.
[9] R.F. Wei, K.J. Li, J.J. Feng, X.L. Tian, Y.F. Shi, X.M. Li, F.F. Hu, H. Guo, J. Am. Ceram. Soc. 103 (2020) 2610–2616.
[10] B. Padlyak, Ukr. J. Phys. Opt. 9 (2008) 51–59.
[11] J. Ueda, A. Hashimoto, S. Tanabe, J. Mater. Chem. C. 44 (2016) 10529–10537.
[12] A.J. Bosman, E.E. Havinga, Phys. Rev. 129 (1963) 1593–1600.
[13] R.D. Shannon, J. Appl. Phys. 73 (1993) 348–366.
[14] X.Q. Song, M.Q. Xie, K. Du, W.Z. Lu, W. Lei, J. Mater. 5 (2019) 606–617.
[15] J. Varghese, T. Siponkoski, M. Nelo, M.T. Sebastian, H. Jantunen, J. Eur. Ceram. Soc. 38 (2018) 1541–1547.